Sustainable Cities and Society 74 (2021) 103195

Contents lists available at ScienceDirect

Sustainable Cities and Society

journal homepage: www.elsevier.com/locate/scs

Trade-off between vegetation CO_2 sequestration and fossil fuel-related CO_2 emissions: A case study of the Guangdong–Hong Kong–Macao Greater Bay Area of China

Zhaohui Luo [a,b], Yanyan Wu [c], Lixuan Zhou [a,b], Qiang Sun [a], Xijun Yu [a,b], Luping Zhu [a,b], Xiaojun Zhang [a,b], Qiaoli Fang [a,b], Xiao Yang [a,b], Jian Yang [a], Mingyi Liang [a,b], Hengjun Zhang [a,*]

[a] South China Institute of Environmental Sciences, Ministry of Ecology and Environmental, Guangzhou 510655, China
[b] State Environmental Protection Key Laboratory of Urban Ecological Simulation and Protection, Guangzhou 510655, China
[c] Guangdong University of Finance & Economics, Guangzhou 510655, China

ARTICLE INFO

Keywords:
Carbon dioxide emissions
Carbon budget
Nighttime light data
Carbon neutrality

ABSTRACT

Carbon neutrality has attracted tremendous attention. Cities contribute the most to CO_2 emissions. However, the contribution of vegetation to fossil-fuel-related CO_2 emissions in urban agglomeration is unclear. Clarifying the trade-off role of vegetation can disaggregate carbon reduction targets down to sub-units to adapt to and even mitigate global warming. In this study, the Guangdong–Hong Kong–Macao Greater Bay Area (GBA), one of the world's largest metropolitan areas, was studied using our proposed inter-calibration method. The results showed that the inter-calibration method is satisfactory and that the EANTLI model effectively decreases the blooming and saturation effects of nighttime light. In addition, fossil-fuel-related CO_2 emissions increased significantly ($P < 0.0001$) in the GBA during 2000–2018, while the variation in CO_2 sequestrations was far lower than that in the increase in emissions. CO_2 sequestrations by vegetation fully offset fossil-fuel-related CO_2 emissions in 2000, while the status reversed after 2001. Our findings illustrate the role of vegetation carbon sequestration in offsetting fossil-fuel-related CO_2 emissions and emphasize the importance of a CO_2 budget. Additionally, the *one city, one policy* strategy is a good choice for further adapting to and mitigating global warming.

1. Introduction

As the global community is focusing on stabilizing the climate and keeping the global temperature increase within 1.5 ℃ in relation to pre-industrial levels (Wu et al., 2020), decreasing carbon emissions and carbon neutrality are attracting enormous attention. However, with the rapid economic growth in the past two decades, the demand for fossil-fuel-related energy has dramatically increased (Zhao et al., 2018), accounting for more than 70% of the total greenhouse gas emissions into the atmosphere (Meng et al., 2017) and becoming the largest factor accelerating global warming (Ou et al., 2015). In addition, the large amount of carbon dioxide (CO_2) emissions has had significant effects on biological, physical, and socioeconomic systems, such as urban heat islands, biodiversity loss, decline in agriculture productivity, and sea level rise (Coutts et al., 2010; Hirano & Yoshida, 2016). Therefore, understanding the status of CO_2 emissions and the capacity of vegetation to absorb CO_2 is considered a fundamental step in developing a CO_2 reduction strategy and achieving carbon neutrality.

China consumes 20% of the global primary energy and generates approximately a quarter of global CO_2 emissions, of which 85% are contributed by city energy usage (Shan et al., 2017). To mitigate the adverse effects of CO_2 emissions on ecosystems, the Chinese government has proposed to decrease CO_2 emissions to 60%–65% below 2005 levels by 2030 (Liu et al., 2020; Zhao et al., 2018), and encourage regions, where conditions permit, to take the lead in achieving a carbon peak and carbon neutrality; and achieved carbon neutrality before 2060. Therefore, the total CO_2 emissions and their spatial distribution are critical for policy-makers to consider when working toward emission reductions and monitoring in high-emission areas (Han et al., 2020b).

Cities are the main energy consumers and contribute 85% of the CO_2 emissions in China (Shan et al., 2017), playing a critical role in mitigating climate change (Yang & Li, 2013). Therefore, research on carbon emissions at the city scale requires further attention (Jiang et al., 2020; Liu et al., 2020; Zhou et al., 2021). In addition, an effective

* Corresponding author.
E-mail address: lzhzsdx@163.com (H. Zhang).

https://doi.org/10.1016/j.scs.2021.103195
Received 12 March 2021; Received in revised form 13 July 2021; Accepted 17 July 2021
Available online 21 July 2021

understanding of the status of city-level CO_2 emissions is urgently required to develop an emission reduction policy and mitigate climate change. With the carbon neutrality goal in mind, it is essential to explore the CO_2 budget in city aggregation areas in order to allow for a robust carbon reduction and sequestration strategy (Wang & Cai, 2017) promoting local sustainability and addressing global climate change.

Many researchers have elucidated the CO_2 emissions of administrative units partly due to the limitations of fossil-fuel-related energy data statistics based either on energy balance table or sectoral energy consumption data or on point source carbon emission data (Gudipudi et al., 2019; Jing et al., 2018; Ribeiro et al., 2019). However, statistical data only provide numerical records of fossil-fuel-related energy consumption for an entire unit, and it is difficult to recognize high-emission hotspots in the unit (Su et al., 2014). To quantify the spatial pattern of CO_2 emissions, satellite data (e.g., the Open Source Data Inventory of Anthropogenic CO_2 Emission (ODIAC)) and other auxiliary data (e.g., nighttime light data) are extensively used with fine resolution. However, some limitations exist in relation to estimating the spatial patterns of CO_2 emissions based on nighttime light data. For example, the well-known blooming and saturation effects restrict the capacity of DMSP-OLS data to determine CO_2 emissions, while NPP-VIIRS data have high gain settings, incurring a lot of background noise (Shi et al., 2014). Additionally, NPP-VIIRS nighttime light data start only from 2012, while DMSP-OLS data are available only from 1992 to 2013. Therefore, it is necessary to combine DMSP-OLS and NPP-VIIRS data to estimate CO_2 emissions over a long time series (Shi et al., 2014). However, due to the difference between sensors and the divergent radiance ranges between DMSP-OLS and NPP-VIIRS nighttime light data, inter-calibration between them is difficult and has recently become one of the most eagerly awaited researches (Bennett & Smith, 2017; Zhao et al., 2019b). Moreover, CO_2 emissions based on nighttime light data are usually identified in lit areas, unlit areas with a high population density, or areas of extensive industrial activity, which can cause some CO_2 emissions to be ignored or impossible to estimate. In addition, the role of vegetation in CO_2 sequestration, which can offset energy-related CO_2 emissions, has been largely neglected, especially in urban agglomeration.

The Guangdong–Hong Kong–Macao Greater Bay Area (GBA) is an agglomeration of cities in China, which was established to strengthen international cooperation. However, there is insufficient literature of the spatial distribution of carbon emissions in the GBA (Lin & Li, 2020; Zhou et al., 2018), and the trade-off role of vegetation in fossil fuel CO_2 emission sequestration in the GBA.

In this study, the spatiotemporal variation of the CO_2 budget (the difference between CO_2 sequestration and CO_2 emissions) based on nighttime light data, fuel-related energy statistical data, and net primary productivity (NPP) were explored in the GBA based on the following questions: Is it possible to inter-calibrate DMSP-OLS and NPP-VIIRS nighttime light data to prolong the time range in estimating CO_2 emissions at a finer scale? How much were the CO_2 emissions and the annual variation in CO_2 emissions from fossil-fuel-related energy consumption in the GBA during 2000–2018? Could the CO_2 sequestration by vegetation in the GBA fully offset fossil-fuel-related CO_2 emissions 2000–2018? This study differs from previous ones in that it first inter-calibrates DMSP-OLS and NPP-VIIRS data to prolong the study period in the GBA, and then the best model is taken to further estimate CO_2 emissions based on decreasing the blooming and saturation effects in nighttime light data. Second, a disaggregated model is applied to allocate regional CO_2 emissions to the pixel scale in both lit and unlit areas. Finally, the CO_2 budget is explored so that policymakers can benefit from developing effective strategies for energy consumption and carbon sequestration to further adapt to and mitigate global warming. Our results will provide a feasible estimation methodology for carbon emissions at a high spatial grid scale. They will also help formulate reasonable emission reduction and vegetation carbon sequestration polices to enhance the local ability for sustainable development and mitigate the impacts of climate change on urban development in order to achieve carbon peak and carbon neutrality in China.

The rest of the paper is organized as follows: Section 2 presents the relevant literature review, Section 3 introduces materials and the methodology, Section 4 describes the results, Section 5 provides a discussion of the results and policy recommendations, and Section 6 presents the conclusions.

2. Literature review

The decrease in CO_2 emissions has attracted enormous attention in recent years, and studies have estimated CO_2 emissions based on energy balance tables (EBTs) or energy consumption data (Haug & Ucal, 2019; Shao et al., 2018). Shan et al. (2017) proposed a set of methods of estimating CO_2 emissions based on EBTs. Jing et al. (2018) scaled down provincial energy consumption and carbon emissions to the city scale in 41 cities based on both provincial EBTs and available city-level socioeconomic data. Zhou et al. (2021) estimated fossil-fuel-related CO_2 emissions and land-use emissions in the Beijing–Tianjin–Hebei urban agglomeration based on EBTs and land-use data. The drawbacks of this method is that abundant and comprehensive of data cannot be easily acquired in ordinary prefecture-level cities (Jing et al., 2018). Therefore, some studies have applied a bottom-up approach to estimating CO_2 emissions by using sectoral energy consumption or point source carbon emission data. Wang et al. (2012) estimated CO_2 emissions using the energy consumption data of six sectors in Chinese mega-cities. Wang et al. (2014) built up a 10-km resolution CO_2 emission gridded data for China based on sectoral energy consumption data. Zhou et al. (2018) estimated CO_2 emissions of the GBA cities and surrounding cities based on sectoral and socioeconomic data by using IPCC territorial emission accounting. Cai et al. (2018) constructed a high-resolution CO_2 emission dataset for China based on point emission sources and other socioeconomic data. However, these methods are time-consuming and require more personnel and material resources (Jing et al., 2018). In addition, the status of social sectors and time scales are inconsistent, and the corresponding data acquired may differ from city to city. Therefore, a comparison of these studies was weak (Shan et al., 2017), and the method cannot be used in other cities (Jing et al., 2018). Moreover, both the two type of methods mentioned above cannot reflect spatial characteristics of CO_2 emissions, especially for uneven development within cities.

With satellite development, there are now many emission analysis products available, such as the China High Resolution Emission Database (CHRED), the Carbon Emission Accounts and Dataset (CEADs), the Multi-resolution Emission Inventory for China (MEIC), the Emissions Database for Global Atmospheric Research (EDGAR), the Fossil Fuel Data Assimilation System (FFDAS), and the Open-source Data Inventory for Anthropogenic CO_2 (ODIAC). Although these data are widely used at global and national scales, they contain large uncertainties (Han et al., 2020a; Wang & Cai, 2017) when applied at the regional or even the city scale due to coarse spatial resolution (e.g., EDGAR and FFDAS have a spatial resolution of 0.1°), discontinuous yearly data (e.g., CHRED and MEIC), or output data that are an emission inventory at the administrative scale, not grid data (e.g., CEADs). Therefore, these data are rarely applied at smaller city scales due to poor accuracy (Jing et al., 2018). The ODIAC has been widely used by the international research community for a variety of research applications (Oda et al., 2018). However, the ODIAC pioneered the combined use of nighttime light data and individual power plant emission/location profiles and was not originally designed to monitor urban CO_2 emissions (Chen et al., 2020a; Oda et al., 2019), so it underestimates the emissions from areas that do not have strong nighttime light (Wang et al., 2013) and overestimates emissions from urban areas (Wang and Cai, 2017). More importantly, the statistical data used are not the city's own statistical data, increasing the uncertainty of the results.

In summary, due to insufficient basic data at the city level, a few of the methods mentioned above can be applied to estimate CO_2 emissions

of cities at the grid scale due to uneven development between or within cities, despite an urgent need for better understanding of city-grid-scale CO_2 emissions to make corresponding policies (Jing et al., 2018; Lin & Li, 2020). In addition, China has pledged to achieve carbon neutrality before 2060, and vegetation carbon sequestration is a critical way to achieve carbon neutrality. However, studies on net carbon emissions in China are lacking (Han et al., 2017), especially for urban agglomerations. Taking full account of previous studies and data availability, in this study, we proposed a feasible method of estimating city CO_2 emissions at the grid scale based on a city's own statistical data and further explored the role of vegetation in absorbing energy-consumption-related CO_2 emissions.

3. Materials and methods

3.1. Study area

The GBA is located in Southern China (Fig. 1), and is a regional and municipal cluster comprising nine cities (Guangzhou, Zhuhai, Foshan, Zhaoqing, Jiangmen, Shenzhen, Zhongshan, Huizhou and Dongguan) and two special administrative regions (Macao and Hong Kong). Its area is approximately 5.6×10^4 km^2, and the total domestic product and resident population in 2018 reached 1.34 trillion USD and 70 million, respectively, accounting for 12% of the country's total economic output (Chen et al., 2020b).

Image deleted. Please check.Image deleted. Please check.Image deleted. Please check.Image deleted. Please check.Image deleted. Please check.Image deleted. Please check.Image deleted. Please check.Image deleted. Please check.Image deleted. Please check.Image deleted. Please check.Image deleted. Please check.Image deleted. Please check.Image

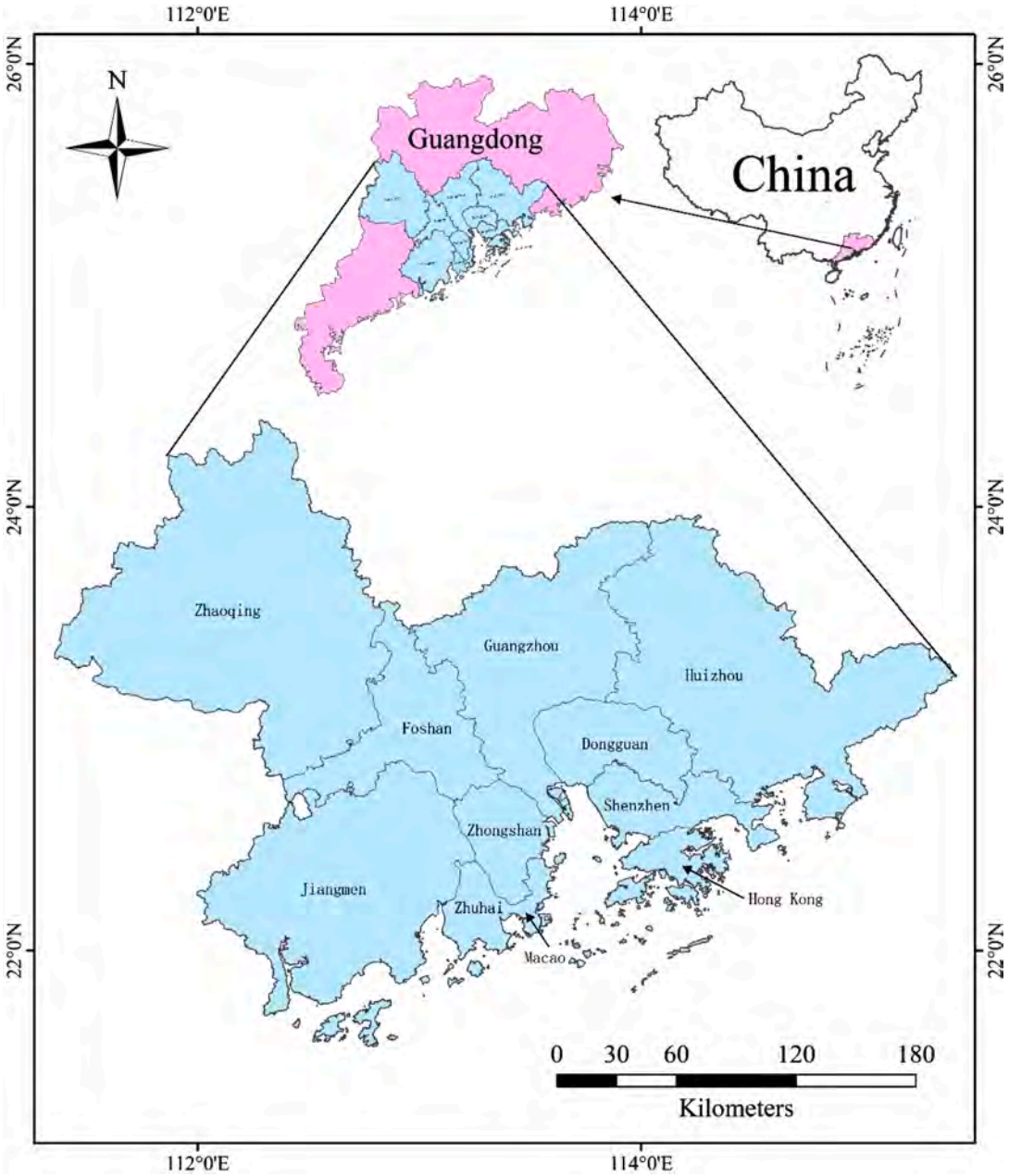

Fig. 1. Location of the GBA.

deleted. Please check.

3.2. Dataset and methodology

3.2.1. Dataset

The dataset applied includes statistics on energy consumption, products of the moderate-resolution imaging spectroradiometer (MODIS) enhanced vegetation index (EVI), and MODIS yearly NPP, population density and nighttime light data (DMSP- OLS and NPP-VIIRS).

Fossil-fuel-related energy consumption data for estimating CO_2 emissions were acquired from the corresponding City Statistical Yearbooks and China Energy Statistical Yearbooks. Considering the availability and limitation of data at the city level, the energy consumption data were mostly statistical based on standard coal. Therefore, total CO_2 emissions in the GBA were calculated using the method proposed by Tu and Liu (2014).

Terra MODIS products, namely, MOD13A3 and MOD17A3H, were downloaded from the Land Processes Distributed Active Archive Center (LP DAAC). MOD13A3 is an EVI product with a temporal and spatial resolution of 1 month and 1 km, respectively, generated since 2000. The quality flag files were first referenced to exclude bad pixels, and the annual mean EVI was calculated to decrease the sensitivity of seasonal and inter-annual fluctuations (Zhang et al., 2013). Finally, pixels with an EVI value of less than 0 were removed to further mask non-vegetation (Luo et al., 2018a). The yearly NPP products (MOD17A3H) with a spatial resolution of 0.5 km × 0.5 km were reprojection and imagery clipping and were resampled to 1 km ×1 km. We validated MODIS NPP with a forest resource inventory in Guangdong Province (Fig. S1), with acceptable results (Fig. S2).

Population density grid data, with a spatial resolution of 1 km for 2000, 2005, 2010 and 2015, were obtained from the Data Center for Resources and Environmental Sciences (RESDC), Chinese Academy of Sciences. The dataset was generated based on demographic statistics at the county level by spatial interpolation, and the value of each pixel was the population count as an integer.

Two types of nighttime light data, namely, DMSP-OLS version 4 datasets from 2000 to 2013 and NPP-VIIRS datasets from 2012 to 2018, were downloaded from the National Geophysical Data Center (NOAA/NGDC). DMSP-OLS datasets are cloud-free composites from which noises (e.g., gas flares) have been removed. Since the data were generated from different DMSP satellites, the method proposed by Cao et al. (2015) was applied for calibration. Unlike DMSP-OLS data, the noises in the NPP-VIIRS data are not filtered, and negative DN values exist in the original NPP-VIIRS data; therefore, pixels with negative values are excluded (Shi et al., 2014). An annual synthesis of NPP-VIIRS data was carried out and resampled to 1 km × 1 km.

3.2.2. Methodology

3.2.2.1. Inter-calibration between DMSP-OLS and NPP-VIIRS. There is inconsistency between NPP-VIIRS and DMSP-OLS data in relation to, for example, the dynamic range and luminance distribution (Ma et al., 2020). An inter-calibration should be performed for consistency between the two datasets. First, the coefficients of variation (CVs) of 3 × 3 windows of all the pixels in both DMSP-OLS and NPP-VIIRS data for 2012 were calculated. Second, pixels with a CV value larger than 0.3 were excluded, and the remaining pixels represented radiation-stable areas in the two datasets. An intersection operation was performed between the radiation-stable areas. Third, a power function model (Equation (1)) was applied to build the relationship between radiation-stable areas based on the characteristics of pixel pairs in a scatter plot. In addition, a logarithmic transformation was applied to radiation-stable areas for NPP-VIIRS, and a logistical model (Equation (2)) was used to build the relationship between the transformed NPP-VIIRS and DMSP-OLS data. The determinant coefficient (R^2), residual sum of squares (RSS), and root mean squared error (RMSE) were selected to evaluate the two models, and the best one was selected to inter-calibrate the two datasets.

$$y_1 = \mathrm{a} \times {x_0}^b + c \tag{1}$$

$$y_2 = a + \frac{b-a}{1+e^{(c-x_0)\times d}} \tag{2}$$

where y_1 and y_2 represent DMSP-OLS values in the corresponding radiation-stable areas; x_0 in the two equations represents the original NPP-VIIRS and logarithmically transformed NPP-VIIRS values in the corresponding radiation-stable areas, respectively; and a, b, c, and d are the parameters for estimation.

A nighttime light dataset from 2000 to 2018 was constructed. Since Guangzhou, Shenzhen, Hong Kong and Macao are the most developed cities in the GBA, Theoretically the pixel values of the other areas should not be larger than the maximum value of these four cities. However, if they are, the maximum value will be assigned a new value, which will be the maximum value within the pixel's immediate eight neighbors (Shi et al., 2014).

3.2.2.2. Reduction in blooming and saturation effects on nighttime light data. Due to blooming and saturation effects on DMSP-OLS data in bright areas or the core of cities, especially in developed cities Ou et al., 2015; Zhao et al., 2018), DMSP-OLS data are considered unsuitable for directly estimating CO_2 emissions (Zhao et al., 2018). Therefore, many models, such as vegetation-adjusted nighttime light index (VANUI), the human settlement index (HSI), and the EVI-adjusted nighttime light index (EANTLI), have been used to decrease the blooming and saturation problems of nighttime light data. In this study, these three models (Equations (3)–((5)) were constructed, and the best one was selected to decrease the blooming and saturation effects on nighttime light data.

$$\mathrm{VANUI} = (1 - EVI_{mean}) \times \mathrm{NL} \tag{3}$$

$$\mathrm{HSI} = \frac{(1 - EVI_{mean}) + NL_{nor}}{(1 - NL_{nor}) + EVI_{mean} + NL_{nor} \times EVI_{mean}} \tag{4}$$

$$\mathrm{EANTLI} = \begin{cases} \dfrac{1 + (NL_{nor} - EVI_{mean})}{1 - (NL_{nor} - EVI_{mean})} \times NL, & EVI > 0.01 \\ 0, & EVI \le 0.01 \end{cases} \tag{5}$$

where EVI_{mean} donates the yearly mean EVI; and NL and NL_{nor} represent the original and the normalized nighttime light data, respectively.

3.2.2.3. Estimation of pixel-based CO_2 emissions. To estimate the spatial pattern of CO_2 emissions, a top-down process based on the combination of nighttime lights and population counts in both light areas and non-light areas was applied (Ghosh et al., 2010; Liu et al., 2018; Ou et al., 2015):

(1) The boundary of urban (with light data) and rural (without light data) areas was first identified based on adjusted nighttime light data. To correctly determine the actual boundary, a dynamic threshold method was applied to acquire urban areas based on statistical data of the urban land area from the City Statistical Yearbook. The suitable threshold for determining the urban boundary in the GBA was calculated according to Equations (6) and (7).

$$S_{total} = \sum_{i=DN_{max}}^{DN_{min}} S_{DN_i} \tag{6}$$

$$\left| S_{total}^{DN_i} - S_{stats} \right| \le \varepsilon_{min} \tag{7}$$

where S_{total} is the urban area based on nighttime light data, S_{DN_i} is the total urban area at which the pixel value is higher than DN_i, and S_{stats} is

the actual urban area based on the City Statistical Yearbook. DN_{max} and DN_{min} are the maximum and minimum values of nighttime light data, respectively; DN_i is the one-step value from DN_{max} to DN_{min}; and ε_{min} is the minimum difference between $S_{total}^{DN_i}$ and S_{stats} for all step values from DN_{max} to DN_{min}.

A suitable threshold could be obtained at the point where Eq. (7) was satisfied. The area was divided into two parts according to the threshold, namely urban and rural. The rural area was further divided into a lit area (pixel values of nighttime light data are greater than 0) and an unlit area (pixel values of nighttime light data = 0).

(2) The urban and rural areas with nighttime lights were extracted as a mask to cover the population density grid, and the total population from the lit urban and lit rural areas, namely TP_{Lu} and TP_{Lr}, respectively, were extracted. The remaining part of the area was calculated similarly to obtain the total population in the unlit rural area, namely TP_{Unlr}.

(3) The total CO_2 emissions from the lit urban, lit rural, and unlit rural areas were estimated. The CO_2 emission per capita in the urban area is EPC_{urban} and the CO_2 emission per capita in the rural area is $EPC_{urban} \times x_i$, where x_i is the rural area:urban area ratio of CO_2 emissions per capita. This ratio is equal to 0.08068, 0.0780, 0.0795, and 0.1197 for 2000-2003, 2004-2007, 2008-2012, and 2013-2018, respectively based on the study by Liu et al. (2018) in Guangdong Province. Then, the total CO_2 emissions from the lit urban, lit rural, and unlit rural areas can be expressed as Equations (8)-(10):

$$CO_2^{LU} EPC_{urban} TP_{Lu} \tag{8}$$

$$CO_2^{LR} EPC_{urban} x_i TP_{Lr} \tag{9}$$

$$CO_2^{ULR} EPC_{urban} x_i TP_{Unlr} \tag{10}$$

where CO_2^{LU}, CO_2^{LR}, and CO_2^{ULR} represent CO_2 emissions in the lit urban, lit rural, and unlit rural areas, respectively, and the unit for CO_2^{LU}, CO_2^{LR}, and CO_2^{ULR} is megaton (Mt).

Since the total CO_2 emissions were the sum of the lit urban, lit rural, and unlit rural areas Equation (11)), EPC_{urban} was expressed as Eq. (12) according to Eqs. (8)-((11).

$$TCO_2 CO_2^{LU} CO_2^{LR} CO_2^{ULR} \tag{11}$$

$$EPC_{urban} \frac{TCO_2}{TP_{Lu} + x_i \times TP_{Lr} + x_i \times TP_{Unlr}} \tag{12}$$

where TCO_2 is the total CO_2 emissions (Mt) in the study region.

(4) Finally, CO_2 emissions in the lit area at the pixel level were distributed in proportion to the values of adjusted nighttime light data mentioned above, while CO_2 emissions in the unlit area at the pixel level were distributed in proportion to the population counts Eqs. (13)-((14)).

$$CO_2^{Li} = \frac{CO_2^{LU} + CO_2^{LR}}{Total_{lig}} \times Lig_i \tag{13}$$

$$CO_2^{ULj} = \frac{CO_2^{ULR}}{Total_{Pop}} \times pop_j \tag{14}$$

where CO_2^{Li} and CO_2^{ULj} represent CO_2 emissions in lit and unlit areas of pixel i and j, respectively (Mt); $Total_{lig}$ and $Total_{Pop}$ represent total nighttime light values and total population values in the GBA, respectively; and Lig_i and pop_j represent nighttime light values of pixel i and population values of pixel j, respectively.

3.2.2.4. Trends in CO_2 emissions. The trend in CO_2 emissions during 2000-2018 at the pixel level was calculated based on robust nonparametric Mann-Kendall (M-K) and Theil–Sen median slope analysis, which could avoid autocorrelation in inter-annual time series data (Luo and Yu, 2017). Additionally, these methods present a monotonic trend, and the normal distribution and independence of time series data were not required (Luo et al., 2018a). For details of these methods, the reader can refer to Gocic and Trajkovic (2013).

3.2.2.5. Estimation of the CO_2 budget. A CO_2 budget was calculated based on the difference between vegetation CO_2 sequestration and fossil-fuel-related CO_2 emissions as Equation (15):

$$CO_2^{budget} = \frac{44}{12} \times NPP - CO_2^{fuel} \tag{15}$$

where CO_2^{budget} refers to the CO_2 budget (Mt); 44/12 represents the ratio of the CO_2 molecular weight to the C atomic weight; NPP is the net primary productivity of vegetation (Mt); and CO_2^{fuel} is the CO_2 emissions from fossil-fuel-related energy consumption (Mt).

4. Results

4.1. CO_2 emissions estimated model

According to the relationship between the two kinds of data, a power function model and a logistical model were constructed. As shown in Fig. 2, the determination coefficients (R^2) for the power function and logistical models were 0.937 and 0.967, respectively. Compared with the power function model, R^2 of the logistical model increased by only 0.03, while the residual sum of squares (RSS) decreased by approximately 44.25% (from 539538.888 to 287518.698). In addition, the RMSE of the logistical model (4.081) was decreased by approximately 27% compared with the power function model (5.591). Therefore, the logistical model was more suitable for calibrating the two kinds of data.

To validate the above conclusion, we applied the logistical model to estimate NPP-VIIRS for 2013 and compared the result with the corresponding DMSP-OLS data. The RSS of 2013 was 2.4×10^4, much lower than that of 2012, and was mainly concentrated around 0 (Fig. 3). Additionally, the RMSE of 2013 was 3.603, also lower than that of 2012. Therefore, the logistical model was applied to adjust NPP-VIIRS data from 2014 to 2018; the estimation values of the parameters for the logistical function are presented in Table 1.

To further decrease the effects of blooming and saturation on nighttime light data, three models (VANUI, HSI, EANTLI) were applied and the normalized results are displayed in Fig. 4. The original DMSP-OLS was almost saturated between 112.8°E and 114.0°E. While the VANUI model could help to decrease the saturation in urban areas (23°N, 112.8°E–114.0°E), the improvements were still not as much as expected compared with the other two models. The effects of the HSI and EANTLI models seemed similar. However, the values of the EANTLI model in rural areas (23°N, 112.5°E–112.7°E and 23°N, 114.4°E–114.9°E) were close to zero, with little change, while the values of the HSI model were larger than zero, with fluctuations. This result indicated that the EANTLI model is better than the other two models. Therefore, the logistical and EANTLI models were used to estimate CO_2 emissions in the GBA.

4.2. CO_2 emissions from fuel energy consumption

Spatial patterns of the mean CO_2 emissions from fuel energy consumption, calculated based on nighttime light and population density data in the GBA from 2000 to 2018, are displayed in Fig. 5a. The spatial pattern was uneven, with gradients that decreased from the center to the sides. The highest emissions occurred in the center of the region, for example, in Guangzhou, Foshan, Dongguan and Shenzhen, with values generally higher than 0.03 Mt/km^2. However, the lowest values (less than 0.002 Mt/km^2) occurred in the northeast, northwest, and southwest of the GBA, for example, in Huizhou, Zhaoqing and Jiangmen. The mean CO_2 emissions in the south of the region ranged from 0.002 to 0.03 Mt/km^2 and mainly occurred in Hong Kong, Macao, and Zhuhai. The total CO_2 emissions increased continuously at a significant rate of

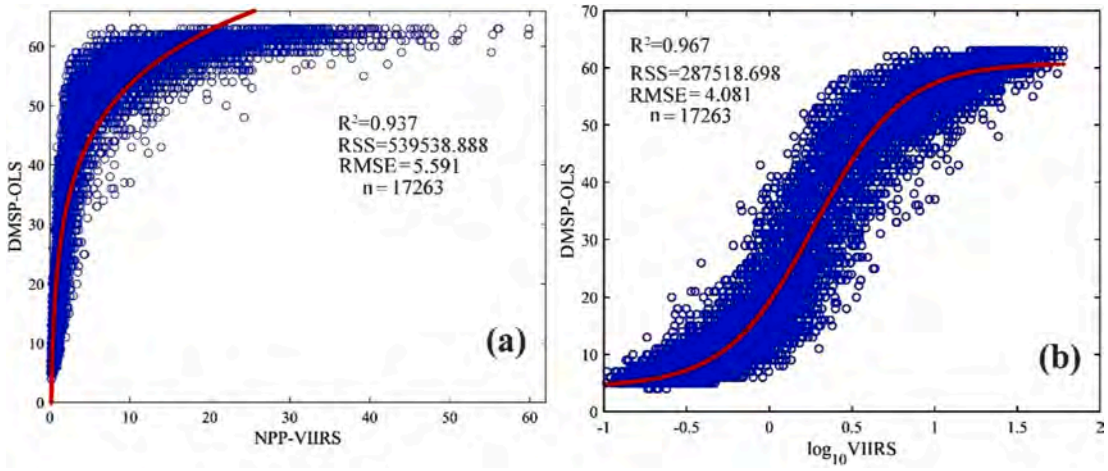

Fig. 2. Scatter plot of the original NPP-VIIRS and DMSP-OLS pixel pairs (a), and a scatter plot of logarithmically transformed NPP-VIIRS and original DMSP-OLS pixel pairs (b) in corresponding radiation-stable areas. The red curves denote the fitted model.

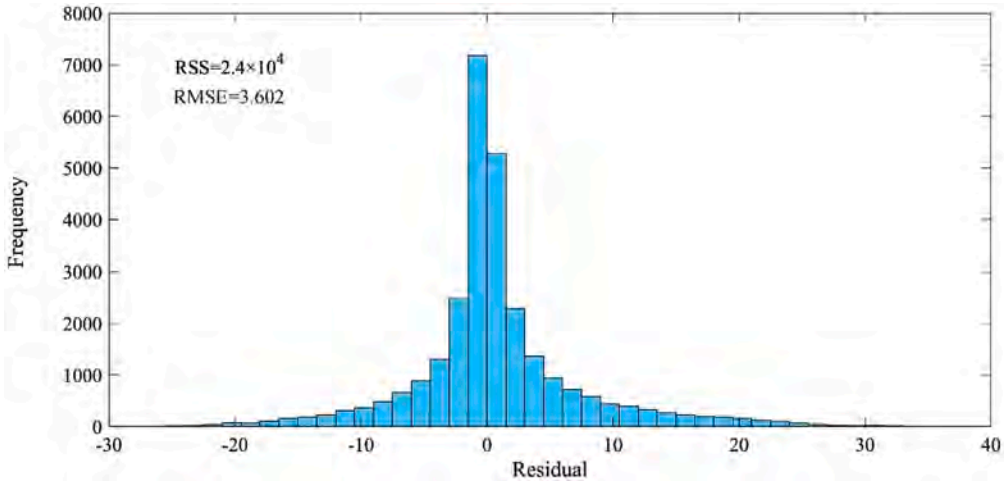

Fig. 3. Frequency distribution of the residual sum of squares between DMSP-OLS and estimated NPP-VIIRS for 2013 based on the logistical model.

Table 1
Parameters of the logistical model

Model	a	b	c	d
Logistical model	4.315	60.851	0.275	3.742

approximately 0.867 Mt/a (P <0.0001).

Fig. 5b details the spatial pattern of the temporal trend in mean annual CO_2 emissions. Over 19 years (2000-2018), more than 81.62% of the total pixels exhibited either significantly decreased or increased trends in the entire region. Areas with a decreased trend only accounted for 1.77% of the total area and mainly occurred in the northwest and northeast, with a decreasing rate of approximately -0.0005 to 0 Mt/km^2. However, more than 98% of the total region showed an increased trend, and approximately 81% had a significantly increased trend ($P < 0.05$), mainly distributed in the center and southeast, with an increasing rate greater than 0.001 Mt/km^2.

To validate the accuracy of the proposed model, a quantitative comparison was performed between the estimated data and actual statistical data. As the model allocated the actual statistical fossil-fuel-related energy of CO_2 emissions to the pixel level in the GBA, the estimated total CO_2 emissions in the GBA from 2000 to 2018 were re-aggregated and compared with the actual statistical data of each corresponding year. Additionally, the averaged CO_2 emissions of each city from 2000 to 2018 were calculated and the total emissions aggregated and compared with the actual statistical data for the corresponding cities. The estimated and actual statistical data showed an almost linear relationship in the GBA, with R^2, mean absolute error (MAE), and RMSE of 0.999, 0.046 Mt, and 0.106 Mt, respectively (Fig. 6a), indicating that CO_2 emissions in the GBA are neither underestimates nor overestimates. In addition, the estimated data at the city level showed a positive, linear relationship with actual statistical data, with an R^2 and mean relative error (MRE) of 0.8791 and 35.0796%, respectively (Fig. 6b). Indicating that the estimated model also performs well at the city scale despite being proposed at the regional scale.

4.3. Carbon sequestration by vegetation

Spatial patterns of the mean annual NPP and annual variation in the total NPP are displayed in Fig. 7. The mean annual NPP showed an increasing trend from the center to the sides. The lowest annual NPP (< 0.579 kg•C /m^2) was mainly distributed in the center and south, in which an impervious surface was mostly distributed under high urbanization. However, an NPP higher than 0.745 kg•C /m^2 occurred in Hong Kong and Macao, which also have high urbanization. By contrast, the highest annual NPP (> 1.236 kg•C/m^2) mainly occurred in the northwest and northeast in areas with high vegetation coverage and relatively low urbanization, compared to Hong Kong or Macao. In terms of the

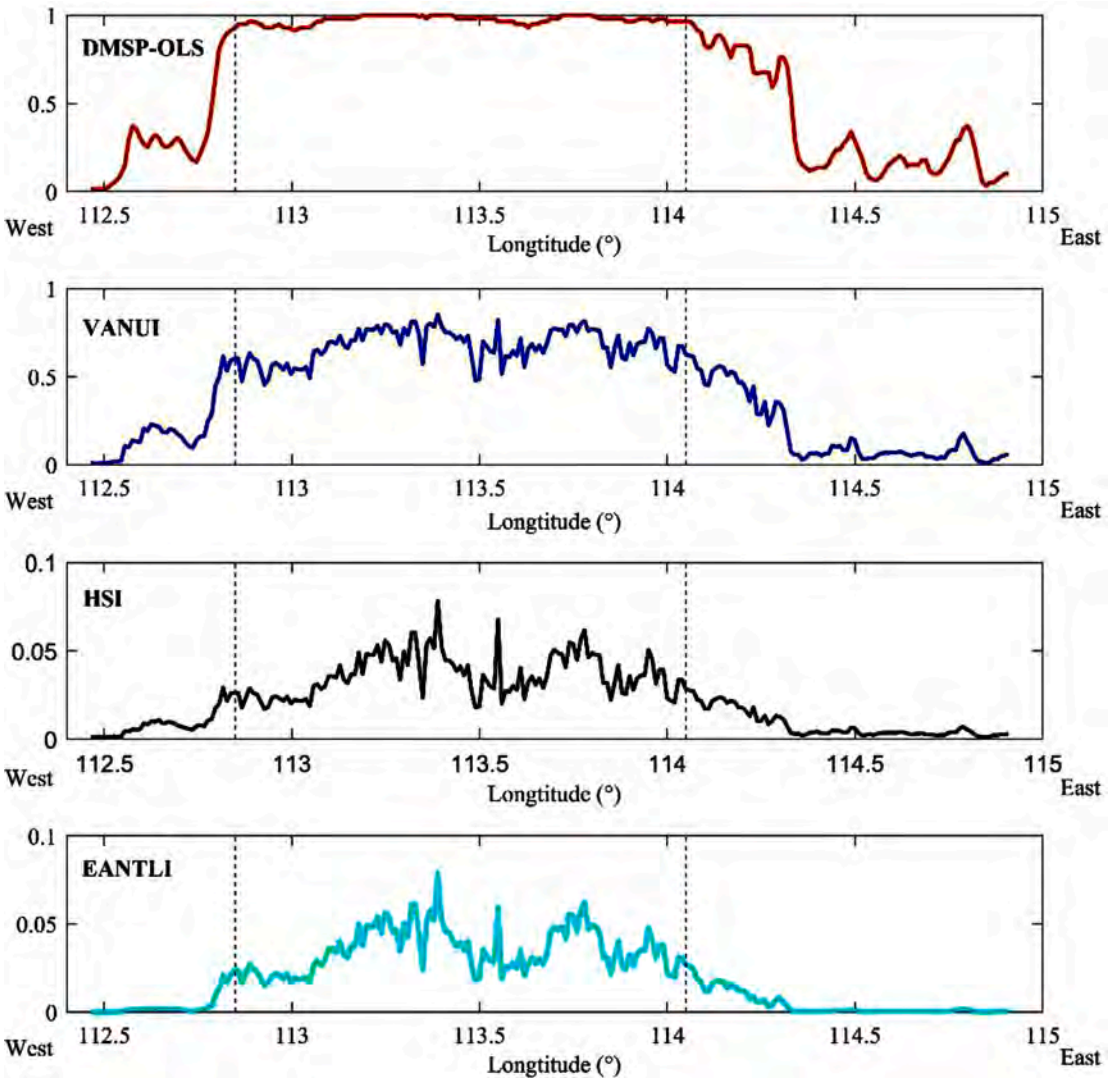

Fig. 4. Latitudinal transects (23° N) of the original DMSP-OLS, VANUI, HIS, and EANTLI performed in the GBA (DMSP-OLS data of 2013 as an example).

temporal variation in the annual total NPP, we found a small fluctuation, with values ranging from 38.75 to 44.65 Mt. While the annual total NPP showed an increasing trend with a magnitude of approximately 0.03 Mt/a, the trend was not significant ($P = 0.664$).

4.4. *Spatiotemporal patterns of the CO_2 budgets*

Regarding the spatial patterns of the CO_2 budget, an increasing trend from the center to the sides can be observed, with three different levels (Fig. 8). The first level was lower than -0.020 Mt/km^2 and was mostly distributed in the center of the GBA. The second level ranged from -0.020 to 0 Mt/km^2 and was mainly distributed in the north of Foshan, Zhongshan, Zhuhai, Hong Kong, and Macao. The third level was greater than 0 Mt/km^2 and was only distributed in most parts of Zhaoqing, Jiangmen, and Huizhou. These results indicated that vegetation in these parts had the ability to fully absorb fossil-fuel-related CO_2 emissions during 2000-2018.

The temporal patterns of the total CO_2 budget displayed a significantly decreasing trend over the study period, with a magnitude of approximately -19.7 Mt/a ($P < 0.0001$). Vegetation in the GBA played a critical role in absorbing fossil-fuel-related CO_2 emissions and could fully offset these emissions in 2000. However, the CO_2 budget changed from positive to negative after 2000 as fossil-fuel-related CO_2 emissions significantly increased (0.867 Mt/a; Fig. 5a), while the NPP increased non-significantly (0.03 Mt/a; Fig. 7) after 2000.

Fig. 9 depicts the CO_2 budget at the city level and shows that CO_2 budgets in Macao, Dongguan, Foshan, Shenzhen, Zhongshan, Zhuhai, Guangzhou, and Hong Kong were all negative from 2000 to 2018. The magnitudes of the CO_2 budget in Guangzhou and Zhuhai showed a continuous downward trend, and the absolute magnitudes of the CO_2 budget became even larger after 2013. By contrast, the negative magnitudes of the CO_2 budget in Dongguan, Foshan, Zhongshan and Shenzhen were mitigated after 2013, indicating the CO_2 sequestration by vegetation cannot fully offset fossil-fuel-related CO_2 emissions in these cities, especially Guangzhou and Zhuhai. For Huizhou and Jiangmen, the CO_2 budget changed from positive to negative value, and the turning point occurred in 2014, indicating that vegetation could fully offset fossil-fuel-related CO_2 emissions in Huizhou and Jiangmen during 2000-2013. However, the status could not be maintained after 2014. The CO_2 budget in Zhaoqing was positive during 2000-2018, indicating that vegetation in Zhaoqing could fully offset fixed-fossil fuel-related CO_2 emissions during the study period. However, this situation is not positive, as the CO_2 budget showed a downward fluctuating trend.

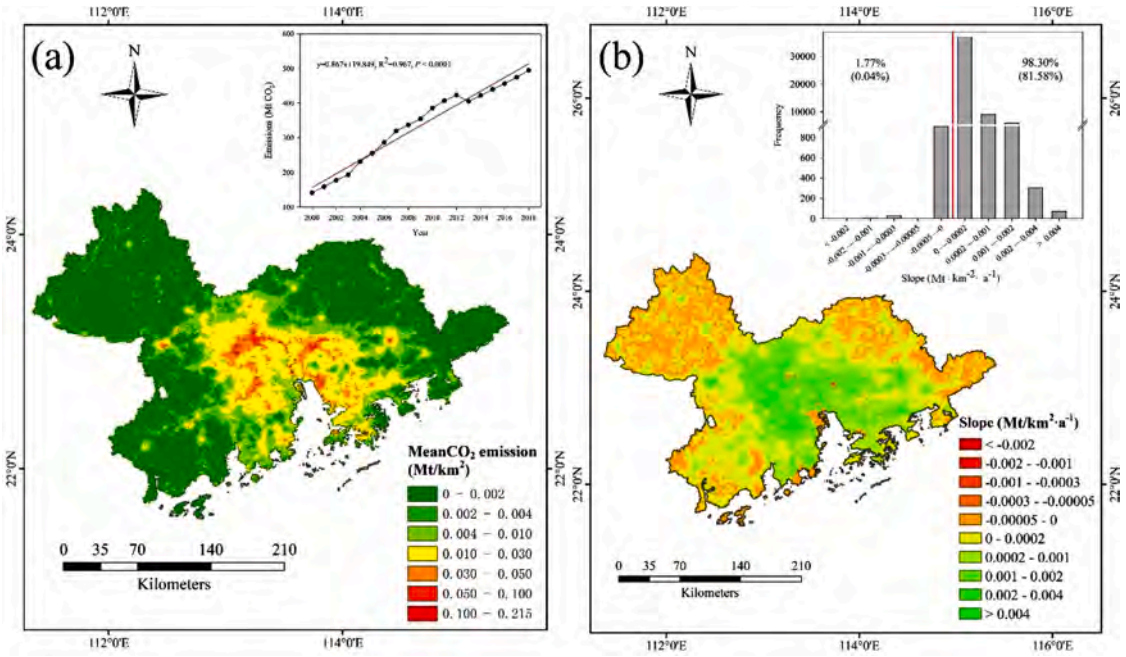

Fig. 5. Spatial distribution **(a)** and annual variation **(b)** of CO_2 emissions in the GBA between 2000 and 2018. The top-right panel in **(a)** represents the dynamics of the total CO_2 emissions from fuel consumption, and the red line indicates the linear fitting. The top-right panel in **(b)** represents the count distributions of the mean annual variation in CO_2 emissions, and the values in parentheses indicate the percentage of pixels with significant trends ($P < 0.05$).

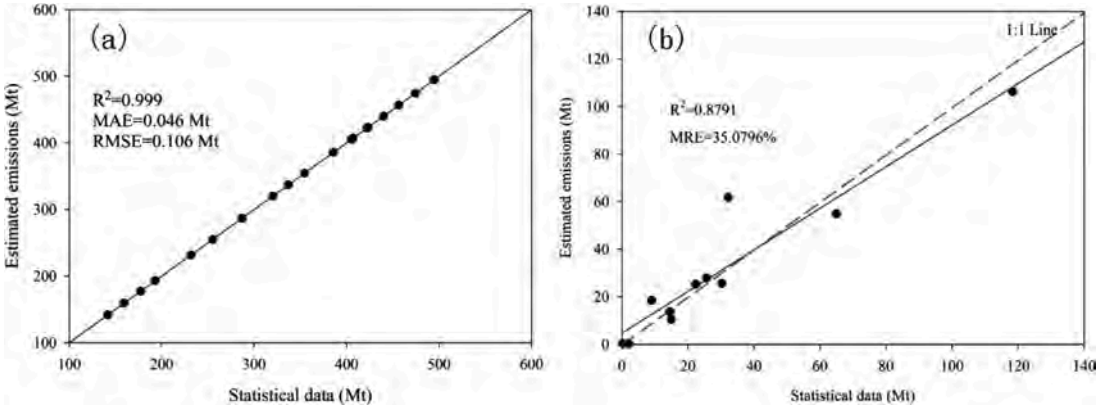

Fig. 6. Comparison of estimated CO_2 emissions and actual statistical CO_2 emissions. (a) Total fossil fuel related-energy CO_2 emissions of 2000-2018 in the GBA and (b) mean fossil fuel related-energy CO_2 emissions of 2000-2018 for 11 cities.

5. Discussion

5.1. Process of nighttime light data

Previous studies have tried to explore the relationship between DMSP-OLS and NPP-VIIRS. Li et al. (2017) applied a power function and convolution to perform an inter-calibration between DMSP-OLS and NPP-VIIRS, and the RMSE was 4.997. Jeswani et al. (2019) applied a logarithm and linear function, and the R^2 was 0.775. Wu and Wang (2019) used a power function and convolution in Beijing and Yiwu, and acquired an RMSE of 9.387 and 7.687, respectively. Ma et al. (2020) compared the linear function, logistical, and BiDoseResp models, and R^2 was 0.847, 0.967 and 0.967, respectively, and the RMSE was 2.847×10^6, 6.199×10^5, and 6.136×10^5, respectively. They concluded that the BiDoseResp model is the best one. Compared with previous studies, our logistical function model in this study is better than the others based on the R^2 and the RMSE.

Light saturation effects limit the correlation between nighttime light data and the estimation of CO_2 emissions and increase the uncertainty in CO_2 emission modeling. Unfortunately, previous studies (Lv et al., 2020; Shi et al., 2016; Su et al., 2014; Wang & Liu, 2017; Wang et al., 2019; Zhao et al., 2019a) have ignored the effects of saturation on nighttime light data during CO_2 emission modeling. Zhang et al. (2013) compared the HSI and the VANUI models to decrease the impacts of saturation on nighttime light data and concluded that the VANUI model significantly decreases the saturation of nighttime light data and is better than the HSI model. Zhao et al. (2018) compared three models (HSI, VANUI, and EANTLI) to reduce the saturation of nighttime light data, and the adjusted R^2 was 0.7102, 0.7548, and 0.7564 for HSI, VANUI, and EANTLI models, respectively, indicating that the VANUI model is better than the HSI model, consistent with Zhang et al. (2013). However, when compared with the EANTLI model, the R^2 of the VANUI model was lower, indicating that the EANTLI model is better in decreasing saturation effects, consistent with Liu et al. (2018), who showed that the EANTLI model is more suitable for CO_2 emission applications than the HSI and VANUI models. Similarly, our results showed that the EANTLI

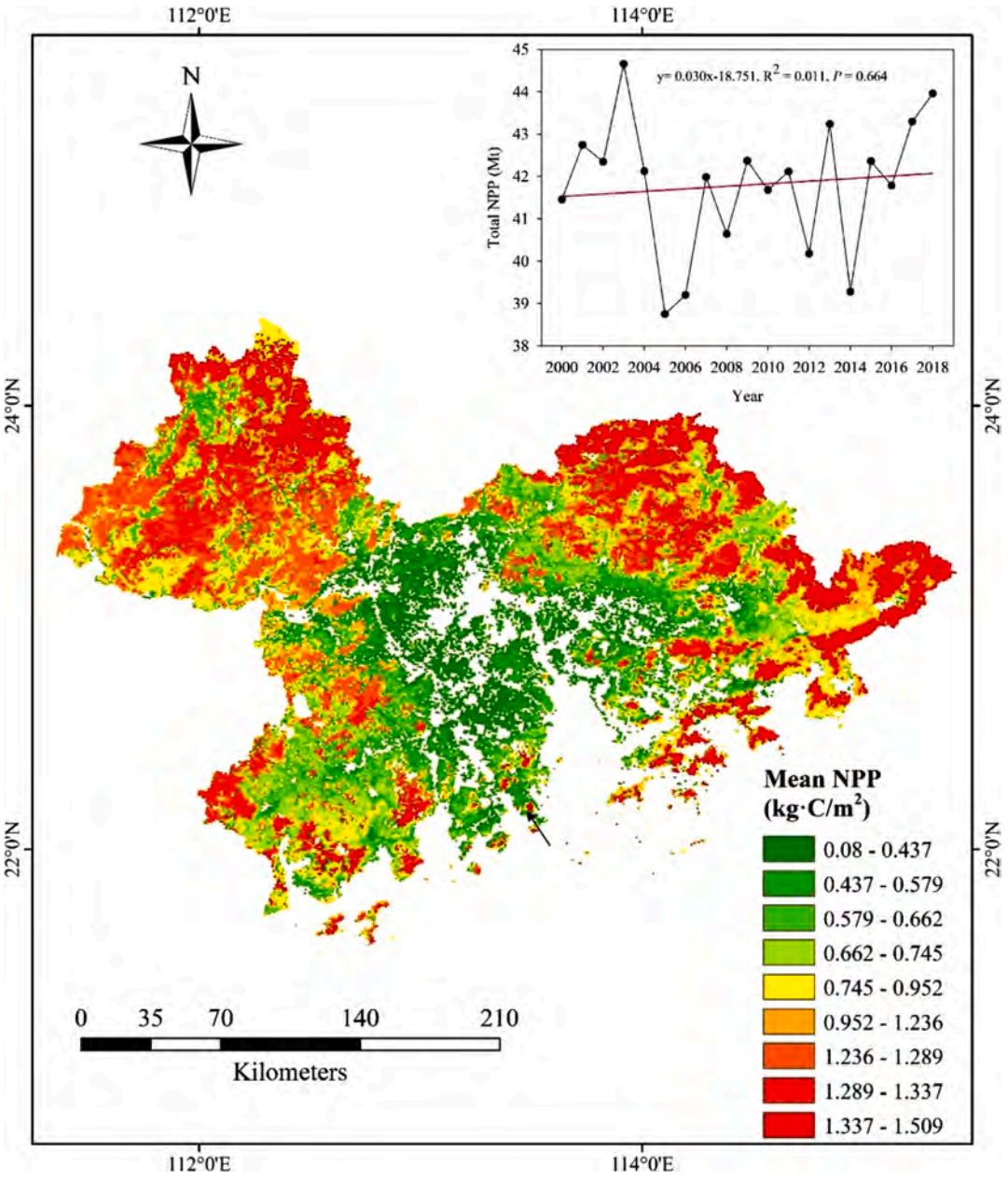

Fig. 7. Spatial pattern of the mean annual NPP during 2000-2018. Inset shows the annual variation in the total NPP in the GBA.

model is better than the other two models in alleviating the saturation problem in both urban and rural areas, which supports the conclusion of previous studies (Liu et al., 2018; Zhao et al., 2018; Zhou et al., 2015).

5.2. CO_2 emissions and sequestration

In this study, we estimated the CO_2 budget in the GBA as the difference between the NPP and fossil-fuel-related CO_2 emissions. With regard to CO_2 emissions, nighttime light data were combined with population data in order to overcome the issue that CO_2 emissions in unlit areas cannot be estimated based only on nighttime light data. We allocated the actual statistical fossil-fuel-related energy of CO_2 emissions to the pixel level, and to validate the result, we compared estimated and actual statistical data at both the regional and the city scale. The estimated and actual statistical data had an almost linear relationship, with the R^2, the MAE, and the RMSE all being satisfactory at the regional scale due to the reason that we allocated the actual statistical fossil-fuel-related energy of CO_2 emissions. Although the R^2 reached 0.999 at the regional scale, and was higher than that achieved by Ghosh et al. (2010), it was a little lower than that achieved by of Liu et al. (2018), which was 1. In terms of validation at the city scale, R^2 and the MRE were 0.8791 and 35.0796%, respectively. Ou et al. (2015) compared actual statistical data with three different emission maps (from NPP-VIIRS and population data, from RCP-DMSP-OLS and population data, and from SLP-DMSP-OLS and population data), and R^2 and the MRE were 0.8695, 0.8386, and 0.7590 and 36.31%, 40.29%, and 52.14%, respectively. Additionally, they compared actual statistical data with three different types of nighttime light data (NPP-VIIRS, RCP-DMSP-OLS, and SLP-DMSP-OLS), and the R^2 and the MRE were 0.8623, 0.8212, and 0.7628 and 36.98%, 41.27%, 52.31%, respectively. Liu et al. (2018) compared estimated and actual statistical emissions based on EANTLI and DMSP-OLS models, respectively, and R^2 value and the MRE were 0.8833 and 0.8182 and 37.92% and 52.35%, respectively. Our evaluation criteria of R^2 and the MRE were better than those of Ou et al. (2015). Although R^2 achieved by of Liu et al. (2018) was a little higher than that of ours, our MRE was lower than that of Liu et al. (2018).

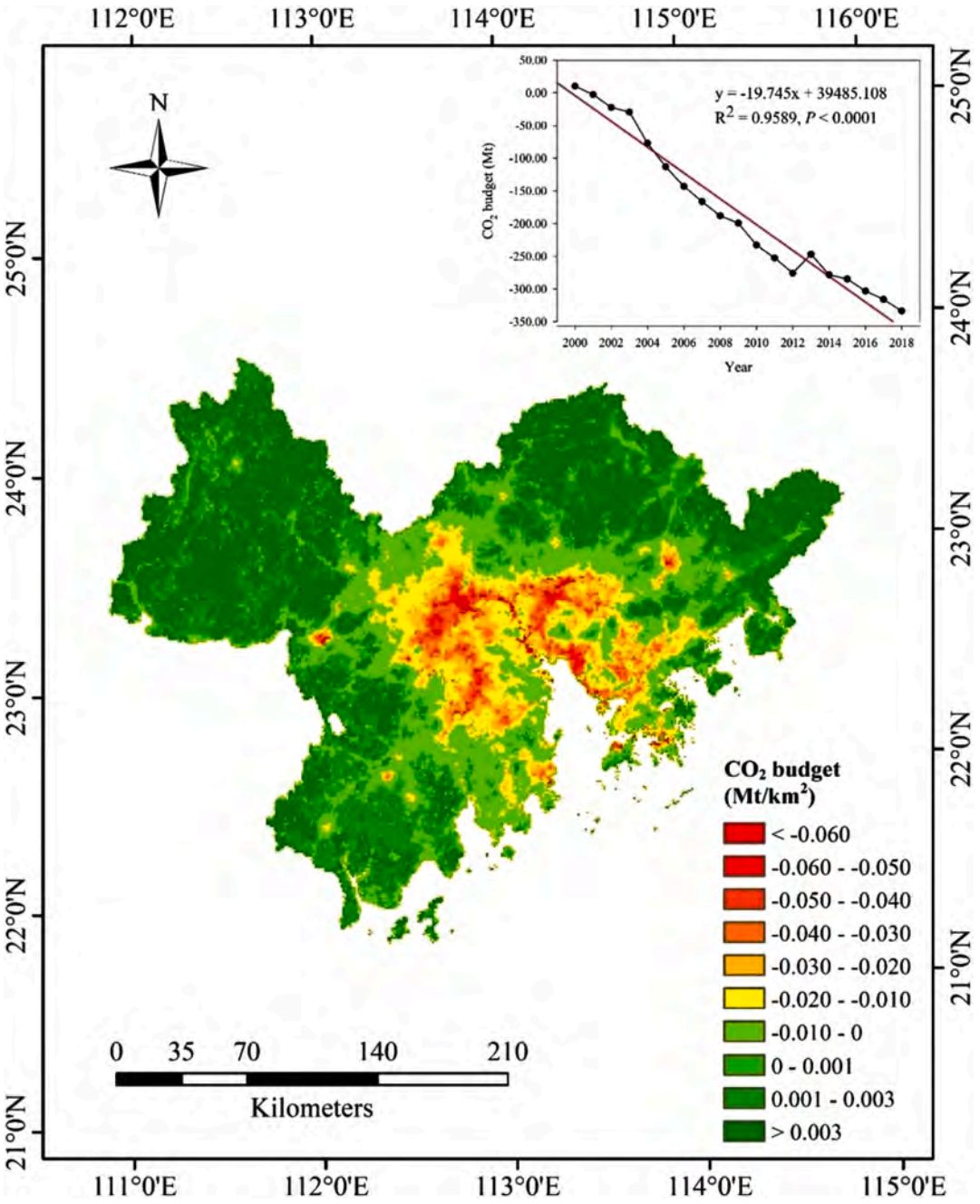

Fig. 8. Spatial pattern of the mean CO_2 budget during 2000-2018. Inset shows the annual variation in the total CO_2 budget in the GBA.

With regard to the spatial distribution of CO_2 emissions, high CO_2 emissions were mainly distributed in urban areas, while lower CO_2 emissions mainly occurred in sub-urban or rural areas, which is consistent with the spatial pattern of economic development and is similar to previous studies (Chuai & Feng, 2019; Wang et al., 2018). At city level, high CO_2 emissions mainly occurred in Guangzhou, Dongguan, and Shenzhen, which are developed or manufacturing cities with an intensive population density or energy consumption. The CO_2 emissions in Guangzhou were 100.45 Mt in 2005 and increased to 132.97 Mt in 2013. Wang et al. (2018) reported that Guangzhou, Dongguan, and Shenzhen had the highest CO_2 emissions in the Pearl River Delta, and CO_2 emissions in Guangzhou increased approximately from 93.45 Mt in 2005 to 127.44 Mt in 2013, similar to our results. Lin and Li (2020) found that CO_2 emissions in Shenzhen and Dongguan were 26.86 and 38.68 Mt, respectively, in 2017, similar to our estimates (27.92 and 49.0 Mt for Shenzhen and Dongguan, respectively). In addition, lower CO_2 emissions were dominant in Zhaoqing, Jiangmen, and north Huizhou, consistent with the result of Wang et al. (2018), and the reason may be the terrain being dominated by mountains and hills and the relatively low economic development level but high vegetation coverage. A significantly increasing temporal trend was found in CO_2 emissions, consistent with Wang et al. (2018), who concluded that most of the Pearl River Delta cities have had a rapid increase in CO_2 emissions in recent decades. Additionally, the high increase mainly occurred in developed areas, indicating that fossil-fuel-related energies were increasingly consumed in developed areas, despite the fact that these areas already have high CO_2 emissions. Moreover, we compared our results with CEADs dataset from 2000-2017 at the city scale (Fig. 10), and result show that the R^2, RMSE and MAE were 0.75, 6.20 Mt and 4.66 Mt, respectively.

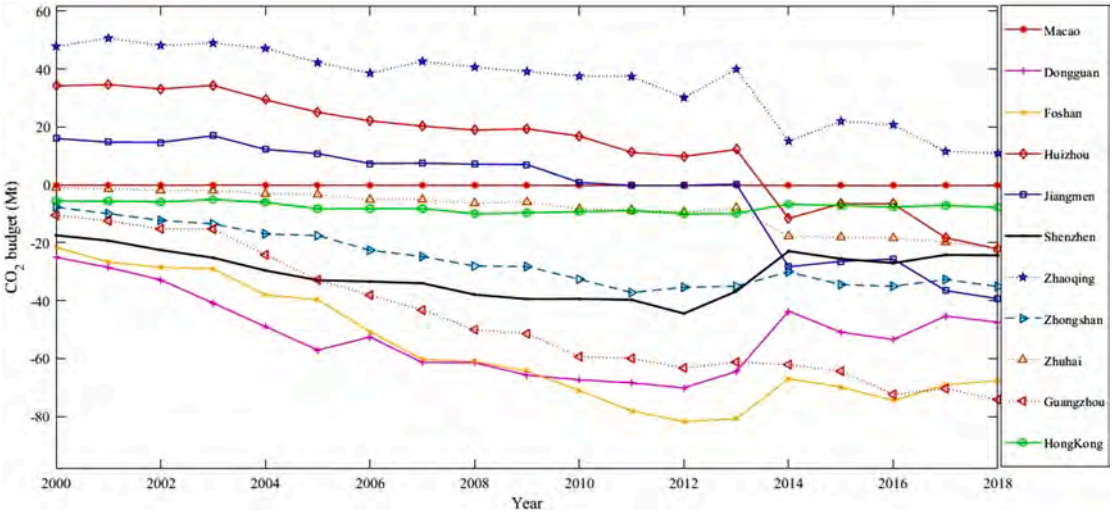

Fig. 9. Temporal trend in the CO_2 budget at the city level in the GBA during 2000-2018.

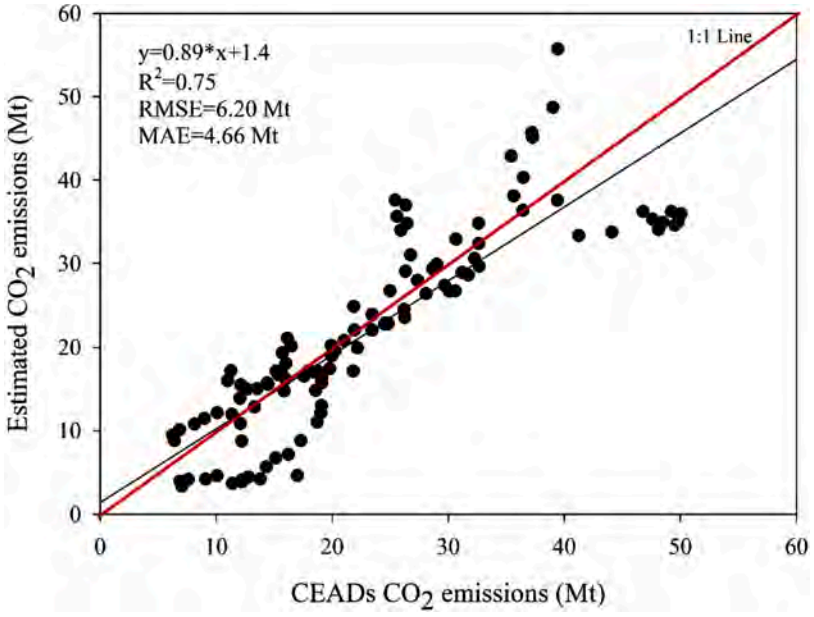

Fig. 10. Comparison of CO_2 emissions between estimated data and CEADs data.

In terms of CO_2 sequestration, the spatial patterns of the NPP with lower values occurred mainly in urban areas and higher values were principally distributed in rural areas. The reason may be anthropogenic activities and the distribution of vegetation coverage. In rural areas, the intensity of development activities or human disturbance is low, favoring vegetation growth and resulting in high vegetation biomass and productivity. In contrast, in urban areas, the effects of disturbance, such as land use and land cover change in ecosystems and soil, are intensive, restraining vegetation growth (Meng et al., 2014).

With regard to CO_2 budgeting at the regional scale, CO_2 sequestration by vegetation could fully offset fossil-fuel-related CO_2 emissions in the GBA in 2000. However, the status could not be maintained at the beginning of 2001, indicating that fossil-fuel-related CO_2 emissions are more than CO_2 sequestration by vegetation, and the absolute difference between CO_2 sequestration by vegetation and fossil-fuel-related CO_2 emissions becomes increasingly larger over the years. The reason is that the majority of CO_2 emissions come from energy consumption and result in a significantly increased trend in CO_2 emissions. However, the NPP increased at a non-significant rate, and the magnitude of NPP variation was much lower than that of CO_2 emissions, indicating that CO_2 sequestration by vegetation alone is not enough to achieve carbon neutrality and the reduction in CO_2 emissions seems more critical CO_2 sequestration by vegetation in the GBA.

CO_2 budgeting at the city scale was a little different from that at the regional scale. CO_2 sequestration by vegetation could not offset fossil-fuel-related CO_2 emissions in Macao, Dongguan, Foshan, Shenzhen, Zhongshan, Zhuhai, Guangzhou, and Hongkong during the study period (2000-2018), while in Huizhou and Jiangmen, vegetation could fully absorb fossil-fuel-related CO_2 emissions during 2000-2013, but the CO_2 budget in Huizhou and Jiangmen became negative during 2014-2018. The CO_2 budget in Zhaoqing was positive during 2000-2018, indicating that vegetation could fully offset fossil-fuel-related CO_2 emissions during the study period. However, this situation is not positive in Zhaoqing due to the downward fluctuating trend in the CO_2 budget. The discrepancy in the CO_2 budget between cities may be due to the difference in economic development that results in different fossil-fuel-related energy consumption and divergent land use and land cover change (Luo et al., 2018b; Wang et al., 2018). These discrepancies

significantly affect both CO_2 emissions and CO_2 sequestration by vegetation. Our results can not only improve our understanding of the spatiotemporal variation in CO_2 emissions, but also offer a reference to allocating CO_2 reduction targets down to each city. Therefore, scientists and government decision makers should pay more attention to the *one city, one policy* strategy to create a CO_2 balance between CO_2 sequestration and CO_2 emissions, especially in the core area of the GBA, such as Guangzhou, Foshan, Dongguan, and Shenzhen, with high CO_2 emissions and low CO_2 sequestration. In addition, focus should be on the CO_2 budget in Zhaoqing, and more efforts such as afforestation, to increase the NPP, and more measures such as renewable energy promotion and application, to decrease fossil-fuel-related CO_2 emissions, should be emphasized to slow down the positive–negative trend in the CO_2 budget.

5.3. Policy implications

Environmental policy formulation cannot be made solely based on CO_2 emissions, but the net CO_2 emissions should also be considered. Therefore, several policy recommendations to decrease CO_2 emissions and increase CO_2 sequestration were proposed.

First, considering the spatiotemporal dynamics of CO_2 emissions in the GBA, a model based on nighttime light data should be established at a regional-city-county scale to provide reliable and refined data. Additionally, a mechanism to decrease CO_2 emissions should be established in regions with high CO_2 emissions, especially Guangzhou, Foshan, Dongguan, and Shenzhen.

Second, the energy-consuming structure plays a vital role in fossil-fuel-related CO_2 emissions. Coal is still the dominant energy source in most cities (Lin & Li, 2020). Therefore, energy system optimization should be prioritized, and fossil fuels should be replaced with cleaner and renewable energy, such as natural gas, nuclear power, offshore wind power, and hydroelectricity, in order to significantly decrease CO_2 emissions (Zheng et al., 2019). Additionally, with the adjustment of the energy-consuming structure, the industrial structure should be gradually transformed from high-energy-consumption industries to high-tech and knowledge-intensive industries as well as modern service industry. Therefore, improved city-level energy and industry structure policies that suit local social-economic conditions should be encouraged. In addition, to realize low-carbon coordinate development with complementary advantages and resource sharing in the GBA, more efforts to break economic, institutional, and technical barriers are required by governments. Cities in the GBA mostly have a mature financial system (Lin & Li, 2020), and a well-established carbon tax system, and well-designed carbon trading and carbon offsetting will promote enterprises to innovate technology and adopt cleaner energy to reduce CO_2 emissions (Lin & Jia, 2019). Finally, public consumer behavior, such as the use of high-tech energy-saving products, conductive to a low-carbon and sustainable lifestyle needs to be encouraged.

Third, areas with high CO_2 emissions usually have a low NPP, which aggravates the current CO_2 budget status in the GBA. Therefore, afforestation programs and a ban on unreasonable deforestation across the region, especially in areas with a low NPP and high CO_2 emissions (e.g., Guangzhou, Foshan, Dongguan, and Shenzhen), should be emphasized. However, some cities, such as Macao, may not have enough space for afforestation. Therefore, it would be better to build an inter-city cooperation mechanism in the GBA to achieve a positive CO_2 budget. Areas with a high NPP and relatively low CO_2 emissions should be maintained to mitigate climate warming and meet the CO_2 emission reduction target, especially in Zhaoqing, whose status may change from a positive to a negative CO_2 budget in the future.

Lastly, the spatial distribution of CO_2 emissions and CO_2 sequestration was divergent between cities. To decrease CO_2 emissions and increase CO_2 sequestration without hampering local economic development, *one city, one policy* may be an ideal strategy. Mature cities should focus more on improving energy efficiency and change the emission trajectories. Other developing cities should make policies according to their sustainable growth principles. For instance, improving energy efficiency in Guangzhou and Shenzhen is more vital than increasing CO_2 sequestration because CO_2 sequestration by vegetation alone cannot achieve carbon neutrality. In contrast, in Zhaoqing, due to its high CO_2 sequestration capacity and low CO_2 emission status, the increase in CO_2 sequestration is more critical than the decrease in fossil-fuel-related CO_2 emissions. Moreover, the establishment of a CO_2 emission market or CO_2 offset market could be considered to compensate cities with low CO_2 emissions.

5.4. Limitations

Due to the limitations of fossil-fuel-related energy data in the City Statistical Yearbooks, CO_2 emissions were converted from standard coal. However, different energies have different average low-order calorific values and carbon emission factors, and the method applied in this study may party increase the uncertainty of CO_2 emissions. Additionally, some factories are distributed in rural areas and also emit a large amount of CO_2, but they only produce these emissions in the daytime. However, these CO_2 emissions cannot be fully detected by nighttime light data and population density data. Other auxiliary data such as land surface temperature may be a good choice to solve this problem. In addition, only CO_2 emissions from fossil-fuel-related energy consumption were estimated in this study, and other CO_2 emission-related processes, such as industrial activities, agriculture activities, and land use and land cover change, should also be considered in the future. Lastly, nighttime light was applied as auxiliary data, but the related sectoral information could not be reflected. Therefore, more efforts have to be made on this issue in the future.

6. Conclusions

This study proposed an inter-calibration method using two kinds of nighttime light data to estimate a city's CO_2 emissions at the grid scale, and the results showed acceptable accuracy compared to previous studies. The method and policy recommendation could be applied to other metropolitan areas, not just in China. Vegetation plays a vital role in assimilating atmospheric CO_2 and could fully offset fossil-fuel-related CO_2 emissions in the GBA in 2000. However, the status could not be maintained after 2000, suggesting it is not enough to sequester CO_2 by vegetation alone in order to achieve carbon neutrality. The decrease of CO_2 emissions seems to be more critical than CO_2 sequestration by vegetation for some cities in the GBA, especially those with high CO_2 emissions (e.g., Guangzhou). Based on our results, *one policy one city* seems an ideal strategy for policymakers to mitigate CO_2 emissions and improve the capacity of CO_2 sequestration to further adapt to and mitigate global warming and also improve the local ability for sustainable development in order to achieve a carbon peak and carbon neutrality in China.

Our method only spatially allocates fossil-fuel-related CO_2 emissions and they are not the full source of CO_2 emissions. For instance, coal power plants are usually distributed far away from residuals, but CO_2 emissions cannot be fully detected by nighttime light data and population density data. Therefore, more efforts should be made in this regard in the future. Additionally, heterotrophic respiration and soil carbon stocks are critical factors that affect the CO_2 budget in the ecosystem, and soil carbon stocks are a vital carbon pool in terrestrial ecosystems. Therefore, these variables should be considered when calculating the CO_2 budget in the future.

Declaration of Competing Interest

The authors declare that they have no known competing financial interests or personal relationships that could have appeared to influence the work reported in this paper.

Acknowledgments

This work was supported by Science and Technology Program of Guangzhou, China (No.201904010288), the National Science Foundation of China (NO.42001214), and Central Fund Supporting Nonprofit Scientific Institutes for Basic Research and Development (No. PM-zx703-201904-139).

Supplementary materials

Supplementary material associated with this article can be found, in the online version, at doi:10.1016/j.scs.2021.103195.

References

Bennett, M. M., & Smith, L. C. (2017). Advances in using multitemporal night-time lights satellite imagery to detect, estimate, and monitor socioeconomic dynamics. *Remote Sensing of Environment, 192*, 176–197.

Cai, B., et al. (2018). China high resolution emission database (CHRED) with point emission sources, gridded emission data, and supplementary socioeconomic data. *Resources, Conservation and Recycling, 129*, 232–239.

Cao, Z., Wu, Z., Kuang, Y., & Huang, N. (2015). Correction of DMSP/OLS Night-time Light Images and Its Application in China. *Journal of Geo-information Science, 17*(9), 1092–1102.

Chen, J., Zhao, F., Zeng, N., & Oda, T. (2020a). Comparing a global high-resolution downscaled fossil fuel CO_2 emission dataset to local inventory-based estimates over 14 global cities. *Carbon Balance Manag, 15*(1), 9.

Chen, Y., et al. (2020b). Relationships of ozone formation sensitivity with precursors emissions, meteorology and land use types, in Guangdong-Hong Kong-Macao Greater Bay Area, China. *Journal of Environmental Sciences, 94*, 1–13.

Chuai, X., & Feng, J. (2019). High resolution carbon emissions simulation and spatial heterogeneity analysis based on big data in Nanjing City. *China. Science of The Total Environment, 686*, 828–837.

Coutts, A., Beringer, J., & Tapper, N. (2010). Changing Urban Climate and CO_2 Emissions: Implications for the Development of Policies for Sustainable Cities. *Urban Policy and Research, 28*(1), 27–47.

Ghosh, T., et al. (2010). Creating a Global Grid of Distributed Fossil Fuel CO_2 Emissions from Nighttime Satellite Imagery. *Energies, 3*(12), 1895–1913.

Gocic, M., & Trajkovic, S. (2013). Analysis of changes in meteorological variables using Mann-Kendall and Sen's slope estimator statistical tests in Serbia. *Global and Planetary Change, 100*, 172–182.

Gudipudi, R., et al. (2019). The efficient, the intensive, and the productive: Insights from urban Kaya scaling. *Applied Energy, 236*, 155–162.

Han, J., et al. (2017). A long-term analysis of urbanization process, landscape change, and carbon sources and sinks: A case study in China's Yangtze River Delta region. *Journal of Cleaner Production, 141*, 1040–1050.

Han, P., et al. (2020a). Province-level fossil fuel CO_2 emission estimates for China based on seven inventories. *Journal of Cleaner Production, 277*, Article 123377.

Han, P., et al. (2020b). Evaluating China's fossil-fuel CO_2 emissions from a comprehensive dataset of nine inventories. *Atmos. Chem. Phys., 20*(19), 11371–11385.

Haug, A. A., & Ucal, M. (2019). The role of trade and FDI for CO_2 emissions in Turkey: Nonlinear relationships. *Energy Economics, 81*, 297–307.

Hirano, Y., & Yoshida, Y. (2016). Assessing the effects of CO_2 reduction strategies on heat islands in urban areas. *Sustainable Cities and Society, 26*, 383–392.

Jeswani, R., Kulshrestha, A., Gupta, P. K., & Strivastac, S. K. (2019). Evaluation of the consistency of DMSP-OLS and SNP-VIIRS night-time light datasets. *Journal of Geomatics, 13*, 98–105.

Jiang, Y., Long, Y., Liu, Q., Dowaki, K., & Ihara, T. (2020). Carbon emission quantification and decarbonization policy exploration for the household sector - Evidence from 51 Japanese cities. *Energy Policy, 140*, Article 111438.

Jing, Q., Bai, H., Luo, W., Cai, B., & Xu, H. (2018). A top-bottom method for city-scale energy-related CO_2 emissions estimation: A case study of 41 Chinese cities. *Journal of Cleaner Production, 202*, 444–455.

Li, X., Elvidge, C. D., Zhou, Y., Cao, C., & Warner, T. A. (2017). Remote sensing of night-time light. *International Journal of Remote Sensing, 38*(21), 5855–5859.

Lin, B., & Jia, Z. (2019). How does tax system on energy industries affect energy demand, CO_2 emissions, and economy in China? *Energy Economics, 84*, Article 104496.

Lin, B., & Li, Z. (2020). Spatial analysis of mainland cities' carbon emissions of and around Guangdong-Hong Kong-Macao Greater Bay area. *Sustainable Cities and Society, 61*, Article 102299.

Liu, X., et al. (2018). Estimating spatiotemporal variations of city-level energy-related CO_2 emissions: An improved disaggregating model based on vegetation adjusted nighttime light data. *Journal of Cleaner Production, 177*, 101–114.

Liu, Z., Wang, F., Tang, Z., & Tang, J. (2020). Predictions and driving factors of production-based CO_2 emissions in Beijing. *China. Sustainable Cities and Society, 53*, Article 101909.

Luo, Z., et al. (2018a). Direct Impacts of Climate Change and Indirect Impacts of Non-Climate Change on Land Surface Phenology Variation across Northern China. *ISPRS International Journal of Geo-Information, 7*(11), 451.

Luo, Z., et al. (2018b). Variation of Net Primary Production and Its Correlation with Climate Change and Anthropogenic Activities over the Tibetan Plateau. *Remote Sensing, 10*(9), 1352.

Luo, Z., & Yu, S. (2017). Spatiotemporal Variability of Land Surface Phenology in China from 2001–2014. In *Remote Sensing, 9* p. 65).

Lv, Q., Liu, H., Wang, J., Liu, H., & Shang, Y. (2020). Multiscale analysis on spatiotemporal dynamics of energy consumption CO_2 emissions in China: Utilizing the integrated of DMSP-OLS and NPP-VIIRS nighttime light datasets. *Science of The Total Environment, 703*, Article 134394.

Ma, J., Guo, J., Ahmad, S., Li, Z., & Hong, J. (2020). Constructing a New Inter-Calibration Method for DMSP-OLS and NPP-VIIRS Nighttime Light. *Remote Sensing, 12*(6), 937.

Meng, L., Graus, W., Worrell, E., & Huang, B. (2014). Estimating CO_2 (carbon dioxide) emissions at urban scales by DMSP/OLS (Defense Meteorological Satellite Program's Operational Linescan System) nighttime light imagery: Methodological challenges and a case study for China. In *Energy, 71* pp. 468–478).

Meng, X., Han, J., & Huang, C. (2017). An Improved Vegetation Adjusted Nighttime Light Urban Index and Its Application in Quantifying Spatiotemporal Dynamics of Carbon Emissions in China. *Remote Sensing, 9*(8), 829.

Oda, T., et al. (2019). Errors and uncertainties in a gridded carbon dioxide emissions inventory. *Mitigation and Adaptation Strategies for Global Change, 24*(6), 1007–1050.

Oda, T., Maksyutov, S., & Andres, R. J. (2018). The Open-source Data Inventory for Anthropogenic CO_2, version 2016 (ODIAC2016): a global monthly fossil fuel CO_2 gridded emissions data product for tracer transport simulations and surface flux inversions. *Earth Syst. Sci. Data, 10*(1), 87–107.

Ou, J., Liu, X., Li, X., Li, M., & Li, W. (2015). Evaluation of NPP-VIIRS Nighttime Light Data for Mapping Global Fossil Fuel Combustion CO_2 Emissions: A Comparison with DMSP-OLS Nighttime Light Data. *PLOS ONE, 10*(9), Article e0138310.

Ribeiro, H. V., Rybski, D., & Kropp, J. P. (2019). Effects of changing population or density on urban carbon dioxide emissions. *Nature Communications, 10*(1), 3204.

Shan, Y., et al. (2017). Methodology and applications of city level CO_2 emission accounts in China. *Journal of Cleaner Production, 161*, 1215–1225.

Shao, L., et al. (2018). Carbon emission imbalances and the structural paths of Chinese regions. *Applied Energy, 215*, 396–404.

Shi, K., et al. (2016). Modeling spatiotemporal CO_2 (carbon dioxide) emission dynamics in China from DMSP-OLS nighttime stable light data using panel data analysis. *Applied Energy, 168*, 523–533.

Shi, K., et al. (2014). Evaluating the Ability of NPP-VIIRS Nighttime Light Data to Estimate the Gross Domestic Product and the Electric Power Consumption of China at Multiple Scales: A Comparison with DMSP-OLS Data. *Remote Sensing, 6*(2), 1705–1724.

Su, Y., et al. (2014). China's 19-year city-level carbon emissions of energy consumptions, driving forces and regionalized mitigation guidelines. *Renewable and Sustainable Energy Reviews, 35*, 231–243.

Tu, H., & Liu, C. (2014). Calculation of CO_2 emission of standard coal. *Coal Quality Technology, 2*, 57–60.

Wang, H., Zhang, R., Liu, M., & Bi, J. (2012). The carbon emissions of Chinese cities. *Atmos. Chem. Phys., 12*(14), 6197–6206.

Wang, J., et al. (2014). High Resolution Carbon Dioxide Emission Gridded Data for China Derived from Point Sources. *Environmental Science & Technology, 48*(12), 7085–7093.

Wang, M., & Cai, B. (2017). A two-level comparison of CO_2 emission data in China: Evidence from three gridded data sources. *Journal of Cleaner Production, 148*, 194–201.

Wang, R., et al. (2013). High-resolution mapping of combustion processes and implications for CO_2 emissions. *Atmos. Chem. Phys., 13*(10), 5189–5203.

Wang, S., & Liu, X. (2017). China's city-level energy-related CO_2 emissions: Spatiotemporal patterns and driving forces. *Applied Energy, 200*, 204–214.

Wang, S., Shi, C., Fang, C., & Feng, K. (2019). Examining the spatial variations of determinants of energy-related CO_2 emissions in China at the city level using Geographically Weighted Regression Model. *Applied Energy, 235*, 95–105.

Wang, S., Zeng, J., Huang, Y., Shi, C., & Zhan, P. (2018). The effects of urbanization on CO_2 emissions in the Pearl River Delta: A comprehensive assessment and panel data analysis. *Applied Energy, 228*, 1693–1706.

Wu, D., Lin, J. C., Oda, T., & Kort, E. A. (2020). Space-based quantification of per capita CO_2 emissions from cities. *Environmental Research Letters, 15*(3), Article 035004.

Wu, K., & Wang, X. (2019). Aligning Pixel Values of DMSP and VIIRS Nighttime Light Images to Evaluate Urban Dynamics. *Remote Sensing, 11*(12), 1463.

Yang, L., & Li, Y. (2013). Low-carbon City in China. *Sustainable Cities and Society, 9*, 62–66.

Zhang, Q., Schaaf, C. B., & Seto, K. C. (2013). The Vegetation Adjusted NTL Urban Index: A new approach to reduce saturation and increase variation in nighttime luminosity. *Remote Sensing of Environment, 129*, 32–41.

Zhao, J., Chen, Y., Ji, G., & Wang, Z. (2018). Residential carbon dioxide emissions at the urban scale for county-level cities in China: A comparative study of nighttime light data. *Journal of Cleaner Production, 180*, 198–209.

Zhao, J., et al. (2019a). Spatio-temporal dynamics of urban residential CO_2 emissions and their driving forces in China using the integrated two nighttime light datasets. *Applied Energy, 235*, 612–624.

Zhao, M., et al. (2019b). Applications of Satellite Remote Sensing of Nighttime Light Observations: Advances, Challenges, and Perspectives. *Remote Sensing, 11*(17), 1971.

Zheng, H., et al. (2019). Mapping Carbon and Water Networks in the North China Urban Agglomeration. *One Earth, 1*(1), 126–137.

Zhou, L., Zhang, X., Zheng, J., Tao, H., & Guo, Y. (2015). An EVI-based method to reduce saturation of DMSP/OLS nighttime light data. *Acta Geographica Sinica, 70*, 1339–1350.

Zhou, Y., Chen, M., Tang, Z., & Mei, Z. (2021). Urbanization, land use change, and carbon emissions: Quantitative assessments for city-level carbon emissions in Beijing-Tianjin-Hebei region. *Sustainable Cities and Society, 66*, Article 102701.

Zhou, Y., Shan, Y., Liu, G., & Guan, D. (2018). Emissions and low-carbon development in Guangdong-Hong Kong-Macao Greater Bay Area cities and their surroundings. *Applied Energy, 228*, 1683–1692.